INFLUENCE OF La_2O_3 ADDITION POWDERS WITH DIFFERENT MORPHOLOGY ON MgB_2 SUPERCONDUCTING CERAMIC

D. Batalu[1*], D. Bojin[1], G. Aldica[2], S. Popa[2], P. Badica[2]

[1]*Polytechnic University of Bucharest, Materials Science and Engineering Faculty, Bucharest, 060042, Romania*
[2]*National Institute of Material Physics, Magurele, 077125, Romania*
**e-mail: dan.batalu@upb.ro*

Keywords: MgB_2, spark plasma sintering, addition powder morphology, physical properties

Abstract
Dense superconducting MgB_2 samples with relative density above 90 % were obtained by Spark Plasma Sintering (SPS). Starting composition of the La_2O_3-added samples was $(MgB_2)_{0.975}(LaO_{1.5})_{0.025}$. We used two powders of La_2O_3 with particle size above and below 100 nm. The obtained SPS-ed La_2O_3-added samples can be viewed as composites: chemical substitutions effects are not significant, if any. There are major morphology differences between SPS-ed samples resulting in very different critical current density, J_c. A higher J_c at 5 and 20 K for the entire field range was obtained for La_2O_3 with the average particle size higher than 100 nm. Contrary to other rare earth oxide additions and to literature, addition of La_2O_3 did not improve J_c vs. pristine MgB_2 sample.

1 Introduction

MgB_2 gain an important attention since the discovery of its superconducting properties [1]. Although it is an attractive material due to its lightness, low price and availability enhancement of the superconducting properties, such as current density and irreversibility magnetic field are necessary. Rare earth (RE) elements, their oxides or compounds were added [2-11] to MgB_2.

In this work we used La_2O_3 'nano' powders (nano, <100 nm) and 'micro' powders (μ, >100 nm) as additions to MgB_2. Resulting composites have different critical current density, J_c. They also show differences if compared to pristine MgB_2 sample. Our work indicates that not only the type of the addition, but also the morphology has an important role in controlling the superconducting properties. For samples preparation we used *ex-situ* Spark Plasma Sintering technique (SPS).

2 Materials and testing

Raw materials (Table 1) were MgB_2 and La_2O_3 powders. There are different sizes and shapes of the aggregates and particles (Fig. 1) for the La_2O_3 powders.

MgB_2 and addition powders were manually mixed in an agate mortar. Powder mixtures were loaded into a 2 cm diameter graphite die and processed by SPS (FCT Systeme GmbH – HP D 5, Germany) at 1150 °C for 3 minutes. Heating rate was 160 °C/min. Temperature was monitored with a pyrometer, through an axial hole in the upper punch, ended at 2 mm above

the sample. Uniaxial pressure applied on punches was 95 MPa. The initial vacuum in the furnace was 30 Pa. A pulsed current with a pattern of 12-on/2-off pulses was applied, with a 3 ms period. The total time of one sequence (cycle) was ~ 0.04 s. The operating voltage and the peak current were below 5 V and 1600 A, respectively.

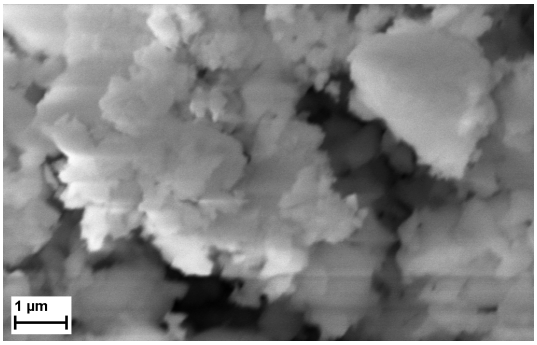

(a)
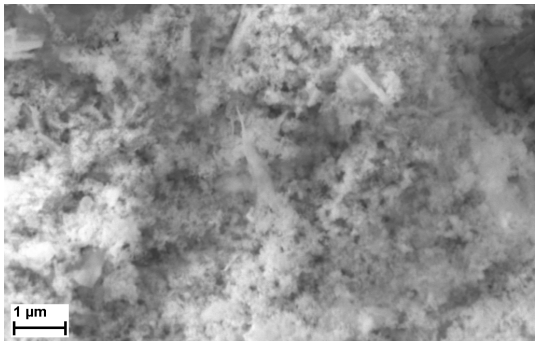

(b)

Fig. 1. SEM images for raw rare earth oxide powders: (a) µ-La_2O_3, (b) nano-La_2O_3.

Raw material	**Average Particle Size (APS), according to the supplier**	**Supplier**	**Purity (%)**	**Addition amount (wt. %)**
MgB_2	1-2 µm (our SEM data show particles < 280 nm)	Alfa Aesar	99.5	-
µ-La_2O_3	100<APS<200 nm	Alfa Aesar	99.99	8.32
nano-La_2O_3	15-30 nm	Chempur	99.9	

Table 1. Some characteristics of the raw powders and their amount as addition in the starting powder mixtures.

Scanning electron microscopy images (SEM-EDS) were taken with Zeiss EVO50 on fresh surface of the fractured samples.

The magnetic moment, *m*, was registered using a commercial Vibrating Sample Magnetometer, VSM (Cryogenic). The external magnetic field, *H*, was applied perpendicular to the largest sample side. The measured samples were parallelepipeds (~ 1.5 x 1.5 x 1 mm^3). All samples were cut from the center of the sintered disc using an oil cooled saw. The *m*(*H*) curves were measured with the magnet in the hysteresis mode. Loops of mass magnetization *m* vs. applied magnetic field *H* were corrected by subtracting the magnetic influence induced by the presence of LaB_6 phase. We consider the *m(H)* values measured on the decreasing branch to determine the critical current density, J_c, using the Bean relation [12] modified for a plate-like geometry (equation 1), [13].

$$J_c = \frac{60 \cdot |m|}{V \cdot \ell} \tag{1}$$

where *m* is the magnetic moment (emu), *V* is the sample volume (cm^3), and ℓ is the basal square side (cm).

3 Results

SEM observation (Fig. 2) reveals samples with two regions. The first one consist of relatively clean MgB_2, composed of dense large blocks (darker regions in backscattering images), and the second one is a matrix rich in La, which surrounds the relatively 'clean' MgB_2. This delimitation into regions is relative, since both regions show different degrees of purity and phase distribution. Very different morphologies of SPS-ed samples lead to different critical

current density.

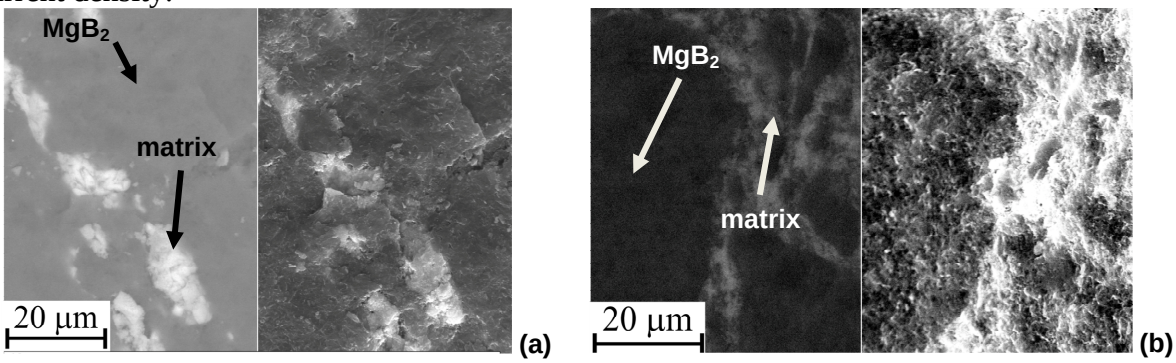

Fig. 2. SEM images for MgB_2 with μ-La_2O_3 (a) and n-La_2O_3 (b) additions.

Curves of the critical current density (J_c) versus magnetic field are shown in Fig. 3. At 5 K the sample with nano-La_2O_3 addition has a lower J_c than the one with μ-La_2O_3 addition. At magnetic fields of about 6 T, both added samples have the same J_c as pristine MgB_2.
At 20 K (Fig. 3.b), again the sample with nano-La_2O_3 addition has a lower J_c than the sample with μ-La_2O_3 addition. At about 3.5 T, the J_c of μ-La_2O_3 added MgB_2 is the same as pristine MgB_2, while the J_c of nano-La_2O_3 added MgB_2 is slightly lower.

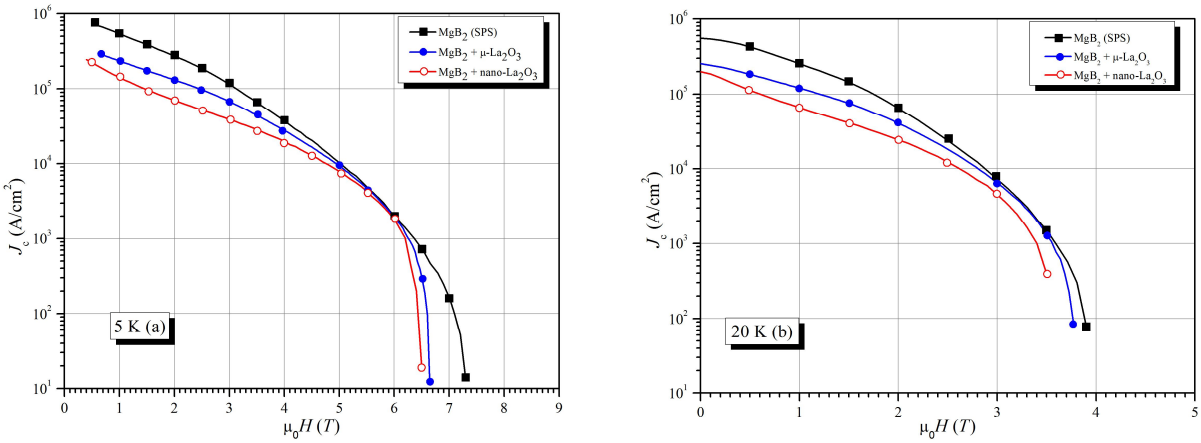

Fig. 3. Critical current density versus magnetic field plots of the pristine and added samples at 5 K (a) and 20 K (b).

4 Conclusions

High density MgB_2 samples added with micro and nano powders of La_2O_3 were obtained by SPS technique. Our samples can be considered composite bulks as observed from the particular morphology revealed by electron microscopy and considering the lack of substitution effects as observed from x-ray diffraction data (not presented).
SPS-ed samples show the enhancement of J_c (at different T and H) for μ-La_2O_3, if compared to nano-La_2O_3 addition. However, both added samples have a lower J_c than for pristine MgB_2.
To explain the different J_c of the SPS-ed samples one has to take into consideration the different morphology of our composite samples induced by the addition raw powder morphology features. We can conclude that not only the addition type is important, but also the morphology features of the additions.

Acknowledgements

D. Batalu recognizes financial support from the European Social Fund through POSDRU/89/1.5/S/54785 project: "Postdoctoral Program for Advanced Research in the field of nanomaterials". G. Aldica and P. Badica acknowledge PCCE 9/2010, Romania.

References

[1] Nagamatsu J., Nakagawa N., Muranaka T., Zenitani Y., Akimitsu J. Superconductivity at 39 K in magnesium diboride, *Nature* **410**, pp. 63-64 (2001).

[2] Kimishima Y., Uehara M., Kuramoti T., Takano S., Takami S. La-doping effects on pinning properties of MgB_2. *Physica C*, **412-414**, pp. 402-406 (2004).

[3] Shekhar C., Giri R., Tiwari R.S., Rana D.S., Malik S.K., Srivastava O.N. Effect of La doping on microstructure and critical current density of MgB_2. *Superconductor Science and Technology*, **18**, pp. 1210-1214 (2005).

[4] Ojha N., Varma G.D., Singh H.K., Awana V.P.S. Effect of rare earth doping on the superconducting properties of MgB_2. *Journal of Applied Physics*, **105**, 315 (2009).

[5] Ojha N., Malik V.K., Bernhard C., Varma G.D. The effect of Pr_6O_{11} doping on superconducting properties of MgB_2. *Physica Status Solidi A*, **207**, pp. 175-182 (2010).

[6] Ojha N., Malik V.K., Bernhard C., Varma G.D. Enhanced superconducting properties of Eu_2O_3 doped MgB_2. *Physica C*, **469**, pp. 846-851 (2009).

[7] Cheng C., Zhao Y. Enhancement of critical current density of MgB_2 by doping Ho_2O_3. *Applied Physics Letters*, **89**, 252501 (2006).

[8] Cheng C., Zhao Y. Significant improvement of flux pinning and irreversibility field of nano-Ho_2O_3 doped MgB_2. *Physica C*, **463-465**, pp. 220-224 (2007).

[9] Varghese N., Vinod K., Chattopadhyay M.K., Roy S.B., Syamaprassad U. Effect of combined addition of nano-SiC and nano-Ho_2O_3 on the in-field critical current density of MgB_2 superconductor. *Journal of Applied Physics*, **107**, 013907 (2010).

[10] Wang J., Bugoslavski Y., Berenov A., Cowey L., Capli A.D., Cohen L.F., Mac Manus Driscoll J.L. High critical current density and improved irreversibility field in bulk MgB_2 made by a scaleable, nanoparticle addition route. *Applied Physics Letters*, **81**, pp. 2026-2028 (2002).

[11] Katsura Y. Shimoyama J., Yamamoto A., Horii S., Kishio K. Effects of rare earth doping on the superconducting properties of MgB_2. *Physica C*, **463-465**, pp. 225-228 (2007).

[12] Bean C.P. Magnetization of hard superconductors. *Physical Review Letters*, **8**, pp. 250-253 (1962).

[13] Gyorgy E.M., Dover R.B., Jackson K.A., Schneemeyer L.F., J.V. Waszczak. Anisotropic critical currents in $Ba_2YCu_3O_7$ analyzed using an extended Bean model. *Applied Physics Letters*, **55**, pp. 283-285 (1989).